Predicting spatial and temporal patterns of soil temperature based on topography, surface cover and air temperature

S. Kang, S. Kim, S. Oh, D. Lee[*]

*Department of Environmental Planning, Graduate School of Environmental Studies,
Seoul National University, Seoul 151-742, South Korea*

Abstract

Soil temperature is a variable that links surface structure to soil processes and yet its spatial prediction across landscapes with variable surface structure is poorly understood. In this study, a hybrid soil temperature model was developed to predict daily spatial patterns of soil temperature in a forested landscape by incorporating the effects of topography, canopy and ground litter. The model is based on both heat transfer physics and empirical relationship between air and soil temperature, and uses input variables that are extracted from a digital elevation model (DEM), satellite imagery, and standard weather records. Model-predicted soil temperatures fitted well with data measured at 10 cm soil depth at three sites: two hardwood forests and a bare soil area. A sensitivity analysis showed that the model was highly sensitive to leaf area index (LAI) and air temperature. When the spatial pattern of soil temperature in a forested watershed was simulated by the model, different responses of bare and canopy-closed ground to air temperature were identified. Spatial distribution of daily air temperature was geostatistically interpolated from the data of weather stations adjacent to the simulated area. Spatial distribution of LAI was obtained from Landsat Thematic Mapper images. The hybrid model describes spatial variability of soil temperature across landscapes and different sensitivity to rising air temperature depending on site-specific surface structures, such as LAI and ground litter stores. In addition, the model may be beneficially incorporated into other ecosystem models requiring soil temperature as one of the input variables. © 2000 Elsevier Science B.V. All rights reserved.

Keywords: Daily soil temperature; Hybrid model; LAI; Spatial mapping

1. Introduction

During the past decades, spatial data of meteorological and soil-physical conditions across landscapes have received much attention. Many studies on spatial patterns of air temperature (Hudson and Wackernagel, 1994; Goward et al., 1994; Willmott and Robeson, 1995; Thornton et al., 1997), precipitation (Daly et al., 1994), humidity (Kimball et al., 1997), available soil water capacity (Zheng et al., 1996), and soil water content (Saha, 1995) have been carried out. Spatial prediction of soil temperature, however, is still a difficult task in spite of its importance in many ecological processes. This is mainly because soil temperature, if measured at all, has rarely been analyzed in relation to structural features although those are necessarily linked to measured data for spatial extrapolation across landscapes. It was reported that root growth and physiological activity of plants, and biological soil activity are largely influenced by soil

* Corresponding author. Tel.: +82-2-880-5650;
fax: +82-2-873-5109.
E-mail address: leedw@snu.ac.kr (D. Lee)

temperature (Kozlowski and Pallardy, 1997). Soil temperature also influences seasonal variation of CO_2 efflux from forest soils (Raich and Schlesinger, 1992; Trumbore et al., 1996; Rochette and Gregorich, 1998; Russell and Voroney, 1998; Striegl and Wickland, 1998). The evidence indicates that the prediction on spatial and temporal patterns of soil temperature will enhance our understanding on the dynamics of vegetation and soil organic matter across landscapes.

In soil heat physics, soil temperature is known as a variable dependent on a number of other variables or parameters, including meteorological conditions such as surface global radiation and air temperature, soil physical parameters such as albedo of surface, water content and texture, topographical variables such as elevation, slope and aspect, and other surface characteristics such as leaf area index (LAI, projected leaf area per unit of ground area) and ground litter stores. Hence, spatial and temporal variation of those variables may be directly linked to soil temperature and thus spatial heterogeneity of biogeochemistry in forested landscape.

Soil temperature might be estimated by two different approaches based upon: (1) soil heat flow and energy balance (Rosenberg et al., 1983; Thunholm, 1990; Marshall et al., 1996), and (2) empirical correlations with easily acquired variables (Zheng et al., 1993). Although the former approach can give accurate predictions for an well-evaluated site, it is difficult to apply across landscapes because of insufficient database for calculating heat transfer equations. Furthermore, temporal patterns of surface global radiation across landscapes necessary for calculating key boundary conditions is difficult to predict in terrain area (Hungerford et al., 1989; Dozier and Frew, 1990; Dubayah, 1992, 1994; Dubayah and Loechel, 1997; Thornton et al., 1997; Antonic, 1998).

On the other hand, empirical regional regression models, such as the one developed by Zheng et al. (1993), require only a few variables such as air temperature and LAI, but depend on good estimates of some key regression coefficients specific to each region. In spite of the limitation, such a site-specific empirical model can be improved when the structure and parameterization process of model are modified in terms of heat transfer physics. Spatial and temporal patterns of key input variables such as air temperature and LAI can be incorporated into a model using

geostatistics (Hudson and Wackernagel, 1994; Willmott and Robeson, 1995; Thornton et al., 1997) and remote sensing (Pierce and Running, 1988; Spanner et al., 1990; Gower and Norman, 1991; Goward et al., 1994; Fassnacht et al., 1997). If spatial information on daily topographic global radiation is not available, this approach may be a promising alternative for predicting spatial and temporal patterns of soil temperature in terrain regions.

The major objective of this study was to develop a robust and easily parameterized model for estimating spatial soil temperature in heterogeneous terrain. The major task was to combine principles of heat transfer physics with an empirical model proposed by Zheng et al. (1993), using spatial data of air temperature and LAI which were generated with geostatistical interpolation and remote sensing, respectively. In the model, elevation is considered as a major topographic variable. LAI and ground litter present important surface characteristics. The model was validated with data collected from three field sites. It is shown that the model can be applied to describe spatial heterogeneity of soil temperature in a forested watershed with heterogeneous topography and vegetation.

2. Development of a hybrid model

2.1. Derivation of damping ratio

Equations that formulate the conduction of heat through a body can be derived from the Fourier equation. The heat transfer equation for a soil matrix is as follows:

$$\frac{\partial T}{\partial t} = \frac{\lambda}{\rho c} \frac{\partial^2 T}{\partial z^2} \tag{1}$$

where T is soil temperature (K), λ the thermal conductivity ($Wm^{-1} K^{-1}$), ρ the soil bulk density (gm^{-3}), c the specific heat capacity of soil ($Jg^{-1} K^{-1}$), z the soil depth (m), and t the time. The value of ρc indicates volumetric heat capacity (JK^{-1}). Eq. (1) can be solved numerically (Becker et al., 1981). Initial and boundary conditions, temperature, and heat flux at soil surface at a given time can be calculated from incident shortwave and longwave thermal radiation (Thunholm, 1990).

Assuming that diurnal and annual temperature variations at soil surface follow a sinusoidal curve, we may employ a known formula of wave function (Eq. (2)).

$$T = T_{avg} + A_0 \sin \omega t \tag{2}$$

where T_{avg} is the mean soil temperature, and A_0 the amplitude of temperature wave at soil surface ($z = 0$). When T approaches T_{avg} with soil depth z, and the thermal diffusivity $\kappa_s = \lambda/(\rho c)$ (m^2 s^{-1}) is constant over time, the solution for Eq. (1) is given as follows (Rosenberg et al., 1983).

$$T(z,t) = T_a + A_0 \exp\left[-z\left(\frac{\omega}{2\kappa_s}\right)^{1/2}\right]$$

$$\times \sin\left(\omega t - z\left(\frac{\omega}{2\kappa_s}\right)^{1/2}\right) \tag{3}$$

Now, a damping ratio of temperature range at a given soil depth can be defined from Eq. (3) by

$$DR_z \equiv \frac{A_z}{A_0} = \exp\left[-z\left(\frac{\pi}{\kappa_s p}\right)^{1/2}\right] \tag{4}$$

where DR_z is the damping ratio at soil depth of z (cm), κ_s the thermal diffusivity (cm^2 s^{-1}), and p the period of either diurnal or annual temperature variation (seconds). A_z and A_0 represent the amplitude of temperature wave at soil depth z and 0, respectively. Eq. (4) implies that in the northern hemisphere soil temperature decreases with increasing soil depth in summer and vice versa in winter. When we use $\kappa_s = 0.004$ cm^2 s^{-1}, $p = 86\,400$ s (1 year), and $z = 10$ cm, for example, the damping ratio of temperature (A/A_0) is ≈0.95, and the soil temperature range at 10 cm depth is ≈5% lower than that at soil surface ($z = 0$).

2.2. Description of the empirical model

Zheng et al. (1993) introduced two empirical equations to estimate daily soil temperature at 10 cm soil depth under vegetation cover using a constant scaling factor, M and the Beer–Lambert law. When $A_j > T_{j-1}$ and when $A_j \leq T_{j-1}$, respectively, mean soil temperature at 10 cm soil depth was estimated by Eqs. (5) and (6):

$$T_j = T_{j-1} + [A_j - T_{j-1}]M \exp[-k\,LAI_j] \tag{5}$$

$$T_j = T_{j-1} + [A_j - T_{j-1}]M \tag{6}$$

where T_j and T_{j-1} are the mean soil temperature under vegetation on the current day and previous day, respectively. A_j represents 11-day mean daily air temperature. An averaging period of 11 days was chosen empirically to reduce the effect of extremes in air temperature. LAI_j represents leaf area index on the jth Julian day, k a extinction coefficient used in the Beer–Lambert Law describing solar radiation interception through the canopy, and M a scaling factor derived from regional regression equations using measured air temperature and soil temperature at 10 cm soil depth. Note that soil temperature on the first simulation day was determined from another regression equation on bare soil (Zheng et al., 1993).

2.3. Hybrid model

We modified the model developed by Zheng et al. (1993) to make it more general. Air temperature and LAI were kept as input variables but we substituted daily air temperatures for 11-day averages. In addition, we replaced the scaling factor, M with a damping ratio (DR_z) to better account for changes in temperature with soil depth. Our model is 'hybrid' in the sense that it incorporates equations describing vertical heat exchange and uses empirical relations between soil and air temperature. During the daytime, net radiative heat transfer occurs downward, while at night, or on cloudy days, the net exchange might be upward through the emission of long-wave thermal radiation. Heat radiation is partly absorbed by ground litter. Our model captures these restrictions on heat exchange by using both LAI and ground litter in the Beer–Lambert Law. Ground litter is given as an equivalent LAI unit and seasonally changes as leaves are shed in the autumn and then decay during the year.

We assumed that soil temperature would not fall below freezing, regardless of the snow depth. This assumption is acceptable in most parts of Korea where snow covers the forest floor during winter. Daily mean soil temperature can be estimated at any depth (z) using the following equations:

When $A_j > T_{j-1}$,

$$T_j(z) = T_{j-1}(z) + [A_j - T_{j-1}(z)]$$

$$\times \exp\left[-z\left(\frac{\pi}{\kappa_s p}\right)^{1/2}\right] \exp\left[-\kappa(LAI_j + Litter_j)\right] \tag{7}$$

and when $A_j \leq T_{j-1}$,

$$T_j(z) = T_{j-1}(z) + [A_j - T_{j-1}(z)]$$

$$\times \exp\left[-z\left(\frac{\pi}{\kappa_s p}\right)^{1/2}\right]\exp[-\kappa \times \text{Litter}_j] \qquad (8)$$

where A_j is mean daily air temperature and Litter_j is LAI equivalent of ground litter. The other variables are the same as above. Note that the initial value of soil temperature is calculated by multiplying DR_z by air temperature of the first Julian day and LAI equivalent of above-ground litter is assumed as a half of the maximum LAI.

3. Application of the hybrid model

Spatial distribution of soil temperature in a forested mountain area, where air temperature data were not available, was predicted with the proposed model by following steps in Fig. 1. At first, georeferenced site-specific air temperatures were estimated from data collected from adjacent weather stations (Step 1). Then, soil temperature was computed from the esti-

mated georeferenced site-specific air temperature and LAI (Step 2). After the model was validated with data collected from different sites (Step 3), a soil temperature map was prepared based on the predictions of the model for each georeferenced site (Step 4).

3.1. Estimation of spatial parameters

Spatial estimates of meteorological conditions have been improved during the last decade for regional analyses as discussed earlier. In spite of the increased computational power, geostatistical methods have been used more often than physically based formulations because the former requires less detailed information. In this study, we apply generalized least-square (GLS) and weighted least-square (WLS) analyses to compare model predictions of soil temperature with measurements. These analyses are relatively simple and easy to apply in terrain regions (Daly et al., 1994; Thornton et al., 1997). Although two simple interpolation methods on air temperature were used in the current study, sophisticated geostatistical methods are available for interpolating air temperature in montane regions (Cressie, 1993; Hudson and Wackerna-
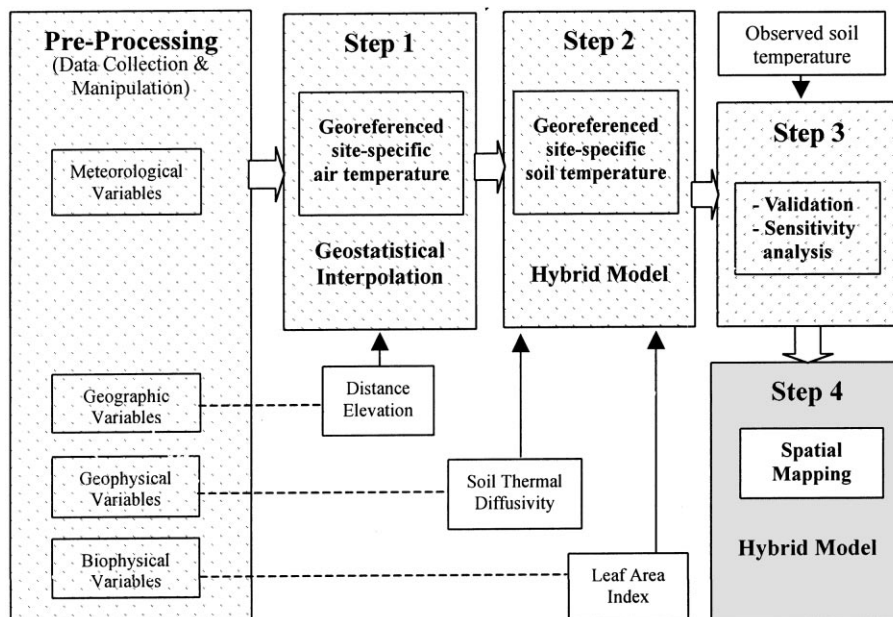

Fig. 1. A schematic diagram illustrating the steps involved in estimating soil temperature from meteorological, topographic, and biologic data.

gel, 1994; Wackernagel, 1995; Kitanidis, 1997; Bellehumeur and Legendre, 1998; Goovaerts, 1998). Among those, kriging with an external drift is one of the prospective examples using digital elevation model (DEM) (Hudson and Wackernagel, 1994). Likewise, spatial variation in LAI can be determined with satellite imagery (Pierce and Running, 1988; Spanner et al., 1990; Gower and Norman, 1991; Deblonde et al., 1994; Goward et al., 1994; Nemani and Running, 1996; Fassnacht et al., 1997). One simple method is to use empirical relationship between vegetation index from satellite image and georeferenced ground-measured LAI.

In the current study, georeferenced analyses were carried out to demonstrate how soil temperature was determined based on the information of topography and vegetation cover across two sub-basins of Mt. Jumbong area using the hybrid model. Based on DEM of 30 m × 30 m resolution, an air temperature map was prepared using GLS method. Spatial distribution of LAI was derived from empirical algorithm between NDVI and LAI. The algorithm was developed by comparing NDVI from TM image on 12 August

1991 and LAI determined with LI-COR 2000 in late August 1998 (Kim et al., unpublished paper).

A sensitivity analysis was employed to determine main influential parameters in model predictability. At last, an example was illustrated to show how soil temperature predictions are distributed across landscapes in relation to topography and vegetation.

3.2. Study area

Three study sites were chosen to validate the model. Two of them are located in the Kangseon Watershed of Mt. Jumbong forest (latitude 38°00′–38°03′N, longitude 128°26′–128°30′E, elevation 700–1424 m, area 1050 ha) in Kangwon Province, South Korea, ca. 200 km east of Seoul and 25 km west of the East Sea (Fig. 2). One site (1000 m above the sea level) represents a hardwood forest dominated by *Quercus mongolica* and *Acer psuedo-sieboldianum* (Lee et al., 1999). The other (800 m above the sea level) lies within a bare soil area where vegetation and surface litter were cleared. The last one (220 m above the sea level) is a deciduous hardwood forest dominated by
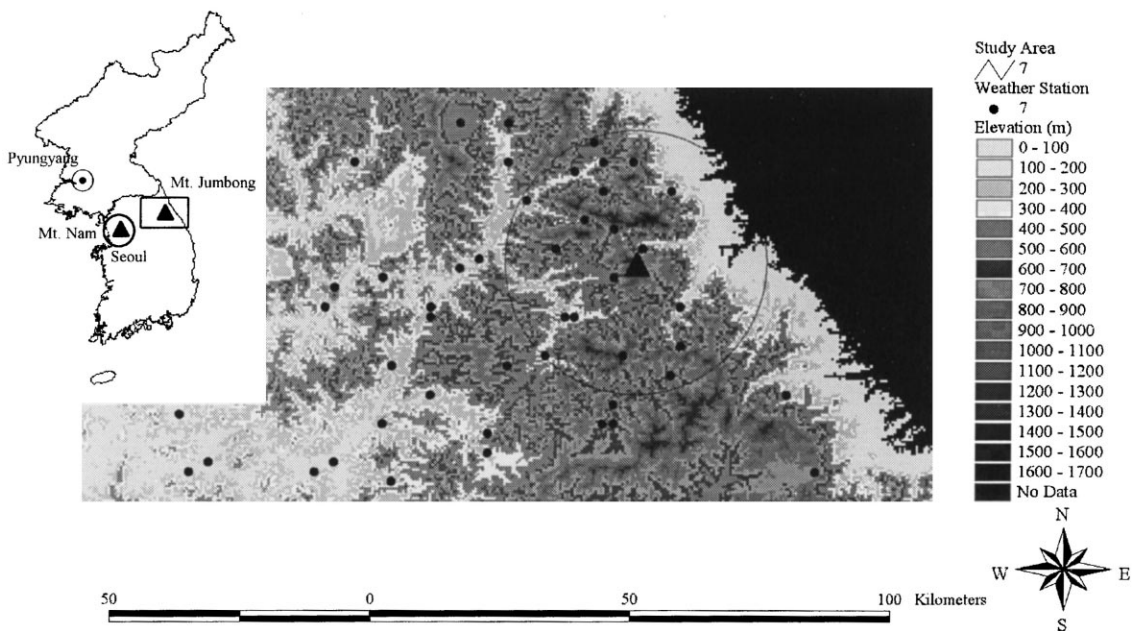

Fig. 2. DEM of the study area (rectangular in keymap). Triangle and solid dots represent the Mt. Jumbong and weather stations where soil and air temperature was collected, respectively. Data from weather stations in a circle within 25 km in radius were used in this study. The cell size in DEM is ≈500 m × 500 m. A keymap in the upper-left corner shows the study sites of Mt. Nam and Mt. Jumbong in South Korea.

Q. mongolica, located in the Mt. Nam forest within the Seoul metropolitan area (Fig. 2).

4. Data collection

Soil temperature has been measured at 10 cm depth using automatic data loggers (Hobo, Onset Computer Corporation) at the hardwood forest site and bare-soil site of Mt. Jumbong since 1996 and 1998, respectively, and at the hardwood forest site of Mt. Nam since 1998. Data were logged hourly from April to December and every 2 h during winter due to inaccessibility under thick snowpack and limited storage capacity of the data logger. Logged data were downloaded every two months (every four months in winter) using Log-book® Software (Onset Computer Corporation) and used for calculation of daily averages of soil temperature (Table 1).

To estimate georeferenced air temperature for Mt. Jumbong forest site where soil temperature was monitored, we used air temperature data from all the weather stations of Korean Meteorological Administration within 25 km in radius (solid dots in Fig. 2). We excluded the data from the stations whose data were missing for more than 18 days ($\approx$5% of a year). As a result, data of six meteorological stations, which are situated from 110 to 771 m above the sea level, were chosen. Short-term missing data were replaced by interpolating with a moving average method. Since April 1998, air temperature data collected hourly were available at the bare-soil site of Mt. Jumbong, using a weather monitoring system (Weatherlink II, Davis Instruments). For the hardwood forest site of Mt. Nam, we used air temperature data collected from a weather station of Seoul (80 m above the sea level), 2.6 km away from the site. In this case, the elevation effect was considered with an assumed temperature lapse rate of -8°C km^{-1}.

Values of LAI were determined at the Mt. Jumbong sites with a LI-COR 2000 Plant Canopy Analyzer from May to August 1998. The combined values of overstory and understory vegetation averaged 5.5 m^2 m^{-2} in late August. A maximum LAI of 5.0 m^2 m^{-2} was assumed for the Mt. Nam forest since a clear-cut area for referencing to open-sky irradiation was not available near the site. It was also assumed that LAI varied sinusoidially during the growing season, reaching the maximum plateau in July.

4.1. Input parameters of the model

The extinction coefficient for the Beer–Lambert law was set at 0.45. Thickness of litter layer was assumed to decrease at a rate of 0.01 per day in unit of LAI equivalent, only when air temperature was above 0°C. The value was $\approx$10-times higher than the decomposition constant of leaf litter observed in the field by a litterbag method in 1996 (Yoo et al., 1999). For the sake of simplicity, the exponential function of litter decomposition at a constant rate was used in this study, but a more reliable model of litter decomposition can be incorporated to enhance predictability in the future. The value of p was given $365 \times 24 \times 60 \times 60$ s to represent annual variation. Soil thermal diffusivity (κ_s) was set at 0.005 cm^2 s^{-1}. For a range of soil texture, the value of κ_s varies from 0.001 to 0.01 cm^2 s^{-1} (Rosenberg et al., 1983; Marshall et al., 1996). This variation is associated not only with soil texture but also with organic matter and moisture content. Within the given range of κ_s, the calculated damping ratio at 10 cm soil depth ranged from 0.93 to 0.97. If soil texture is unknown, a value between 0.93 and 0.97 can be given to estimate seasonal variation of soil temperature. Alternatively, predictions may be improved by considering multiple soil layers with different values of thermal diffusivity (κ_s). The latter approach should be considered if ground is covered with a thick layer of litter or snow (Thunholm, 1990).

Table 1
Summary of site characteristics, soil temperature data, and LAI values collected in late August 1998

Site	Cover	Elevation (m)	Data period	LAI
Mt. Jumbong	None	800	July–November 1998	0
Mt. Jumbong	Hardwood forest	1000	January 1997–November 1998	5.5
Mt. Nam	Hardwood forest	220	March–November 1998	5

5. Results

5.1. Model performance

Soil temperature predicted by the model was compared to data collected from the three study sites at 10 cm soil (Fig. 3). Mean absolute error (MAE) and bias are summarized for each site in Table 2. The
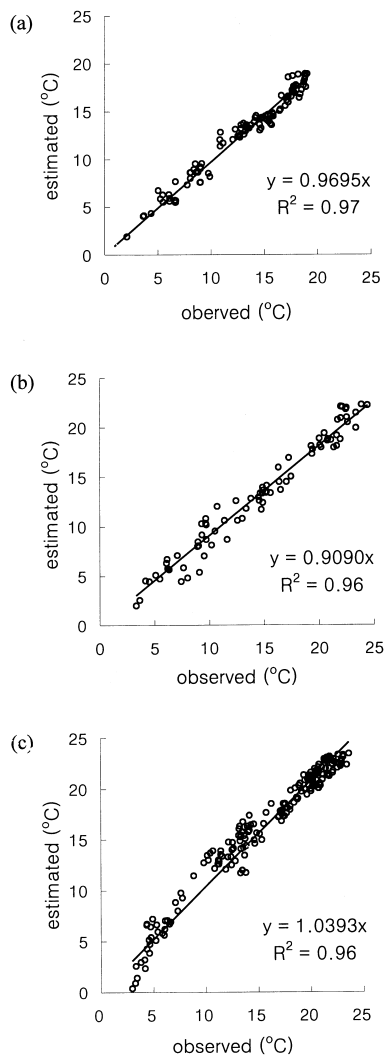

Fig. 3. Relationship between the observed and predicted daily temperature at 10 cm soil depth in 1998 from (a) a hardwood forest of Mt. Jumbong, (b) a cleared area of Mt. Jumbong, and (c) a hardwood forest of Mt. Nam.

hybrid model predicted soil temperature well for the hardwood forest of Mt. Jumbong with MAE of 0.96°C and a bias of 0.03°C. The model was less accurate for the cleared site of Mt. Jumbong with MAE of 1.48°C and a bias of −1.32°C. For the hardwood forest of Mt. Nam, MAE was 1.21°C with a bias of 1.01°C. In all cases, the hybrid model explained >96% of the variation of observed soil temperature.

Site-specific air temperature was estimated from the elevation with general least square (GLS) and from the elevation difference of site and weather stations with inverse-distance weighted least square (WLS). As a result, daily temperature lapse rates averaged −4.9 in GLS and –3.9°C km^{-1} in WLS. The determination of regression averaged 60% in GLS and 30% in WLS. The result led us to employ GLS model when site-specific air temperature was extrapolated from data of weather stations. Time series of the air temperature are presented in Fig. 4.

Using the extrapolated estimates of air temperature, predicted soil temperature was compared among the three alternative models. Daily soil temperatures estimated from the hybrid model (Eqs. (7) and (8)), damping ratio model (Eq. (4)), and empirical model (Eqs. (5) and (6)) were plotted against the data collected from the hardwood forest site of Mt. Jumbong in 1997 (Fig. 5). In terms of mean absolute error and bias, the hybrid model predicted soil temperature better than the others (Table 2). It was also evident in time series of soil temperature that the hybrid model is more reliable than the others. The empirical model suffered from underestimation and
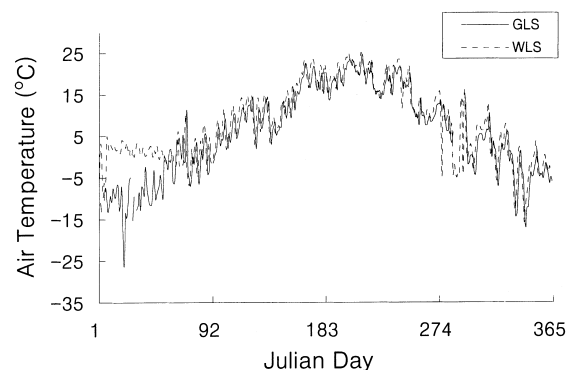

Fig. 4. Estimates of site-specific air temperature at a hardwood forest of Mt. Jumbong.

Table 2
Error analysis and comparisons (mean absolute error (MAE) and bias) for predictive models of soil temperature based on heat transfer physics, empirical correlations, and the hybrid model

Models	Sites	MAE (°C)	Bias (°C)	Required information[a]
Hybrid model	Hardwood forest at Mt. Jumbong	0.96	0.03	
Hybrid model	Bare soil at Mt. Jumbong	1.48	−1.32	T_a, LAI, κ_s
Hybrid model	Hardwood forest at Mt. Nam	1.21	1.01	
Heat transfer model		2.13	0.76	T_a, κ_s
Empirical model	Hardwood forest at Mt. Jumbong	2.07	−1.11	T_{a11}, LAI, M
Hybrid model		1.05	−0.62	T_a, LAI, κ_s

[a] Here, T_a is daily temperature; T_{a11} the air temperature averaged over 11 days; LAI the leaf area index, κ_s the soil thermal diffusivity, and M a scaling factor for regional regressions.

lag effects (Fig. 5d). The underestimation might be attributed to the 11-day running average of air temperature. Although the running average mitigates the effect of extremes and hence is successfully applied for estimating temperature of bare soils (Zheng et al., 1993), it has a redundant effect on soils under canopy.

5.2. Sensitivity analysis

Finally, a sensitivity analysis was carried out for the hardwood-forest site of Mt. Jumbong in 1997 to identify significant parameters and to examine model performance within a range of parameter values. The
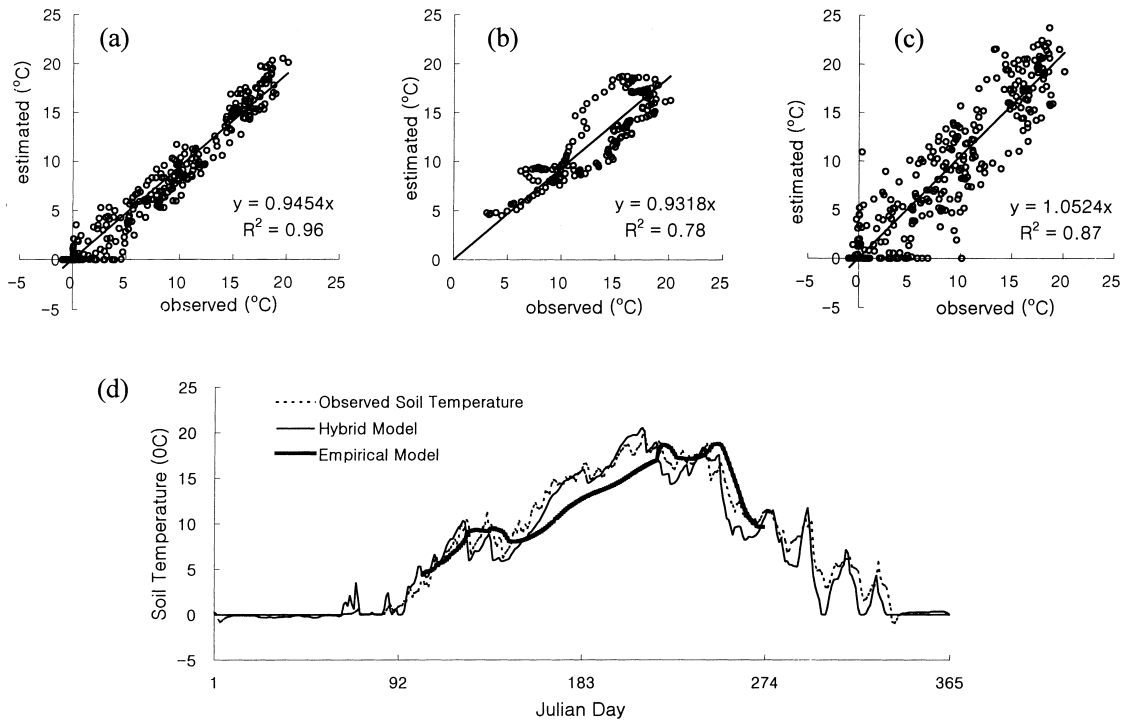

Fig. 5. Relationship between the observed and predicted daily soil temperature at 10 cm soil depth with (a) Hybrid Model, (b) Empirical Model, and (c) Damping Ratio Model. Time series of the observed and predicted soil temperature are compared in (d).
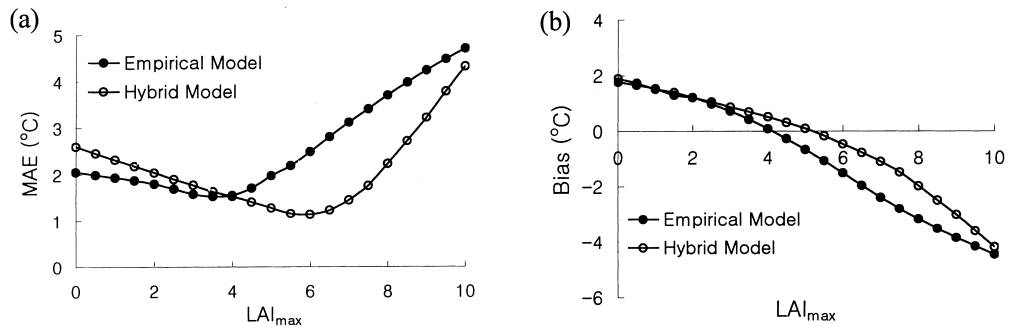
Fig. 6. Comparisons of (a) mean absolute errors (MAE) and (b) bias for the Hybrid Model and Empirical Model based on 1997 data from a hardwood forest site of Mt. Jumbong.
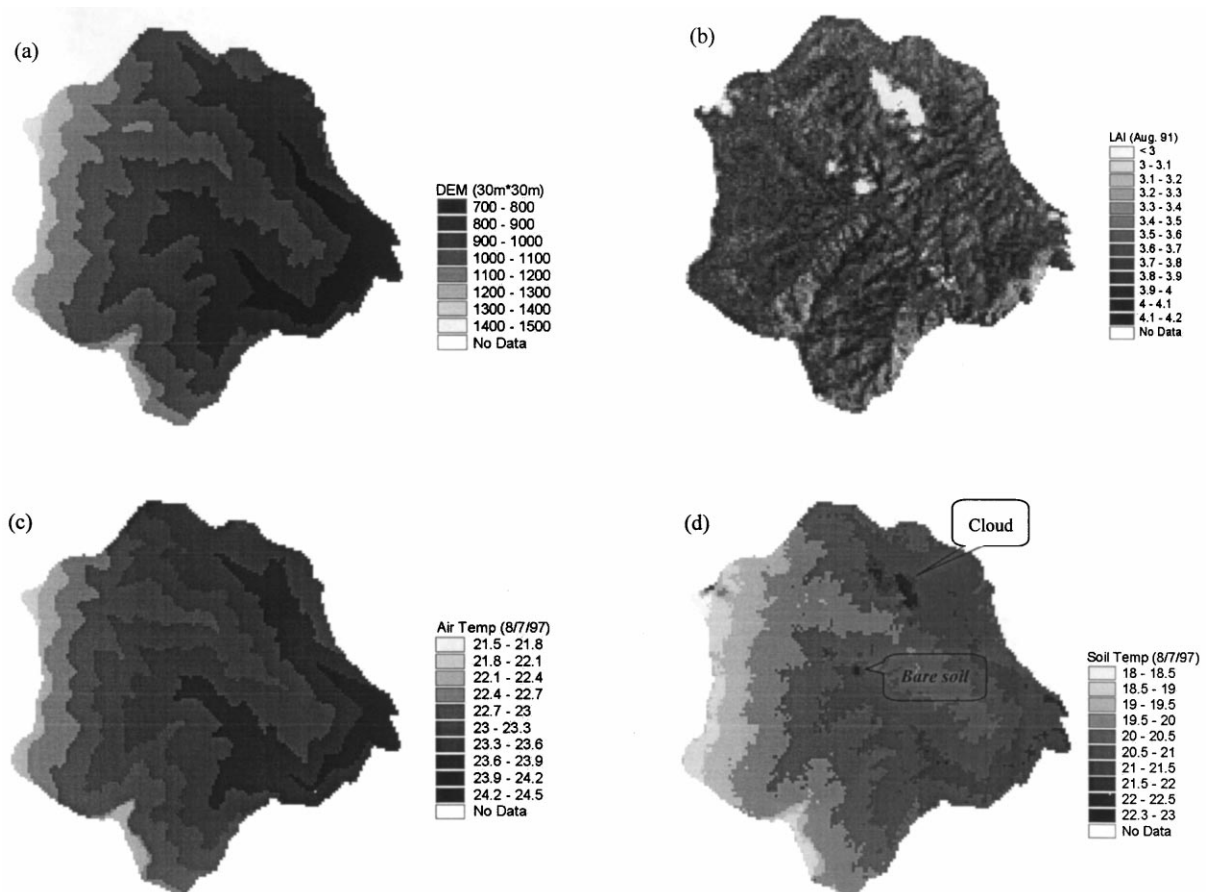

Fig. 7. Demonstration of spatial mapping on soil temperature at 10 cm soil depth in the Kangseon Watershed of Mt. Jumbong forest (1050 ha): (a) DEM of 30 m × 30 m spatial resolution; (b) LAI estimated from TM image on August 1991; (c) an air temperature map derived using a GLS interpolation method on 7 August 1997; (d) a map of daily soil temperature predicted with the hybrid model at 10 cm depth. We used here an empirical algorithm to obtain the LAI map, LAI = 4.7227NDVI + 0.6386 (R^2 = 0.62), developed by Kim et al. (in preparation).

three parameters, i.e., maximum LAI, decay rate of LAI-equivalent ground litter, and thermal diffusivity (κ_s), were considered for sensitivity analysis because those are the only site-specific model parameters that vary with vegetation and soil characteristics. Soil temperature was most sensitive to maximum LAI. As maximum LAI increased from 0 to 10 $m^2 \, m^{-2}$, mean absolute errors (MAE) changed from 1.55 to 4.71°C in the empirical model and from 1.01 to 4.32°C in the hybrid model (Fig. 6a). The bias varied from 2 to −4°C for both of the models (Fig. 6b). Decay rate of LAI-equivalent ground litter had an intermediate effect on model performance during restricted periods before and after the growing seasons and the model was not very sensitive to thermal diffusivity (κ_s) in terms of MAE and bias (not presented here). The improved performance of the hybrid model is evident again as seen in Fig. 6.

6. Discussion and conclusions

Our primary goal was to improve spatial and temporal prediction of soil temperature using a minimum set of variables that can be acquired from weather records, satellite imagery, and digitized elevation maps. The hybrid model was developed to estimate soil temperature by taking into account thermal damping ratio and solar radiation interception by forest canopy and ground litter (or snow). The hybrid model requires no regional regression coefficients and less stringent data but gives better prediction of daily soil temperature than an empirical model reported previously (Zheng et al., 1993).

When the hybrid model is applied at a remote area, spatial mapping on air temperature and LAI is required. Fig. 7 shows a sample application of the hybrid model. Each layer was prepared with the hybrid model following the methods described earlier. Soil temperature showed much more complex pattern than did air temperature (Fig. 7(c and d)), and soil temperature on bare soil was comparably high as expected (Fig. 7d). It shows that with the information of spatially distributed air temperatures and LAI, the hybrid model can predict soil temperature patterns across landscapes. The predictions can be used to estimate spatial variation in soil respiration or organic matter turnover.

On the other hand, soil temperature varied with aspect and slope of soil surface due to different amount of radiative heat flux (Iqbal, 1983; Monteith and Unsworth, 1990; Dubayah, 1997). An illustrative case was found when soil temperature was monitored on the south- and north-facing slope of the hardwood forest site of Mt. Jumbong (Kang et al., unpublished data). In spring and autumn, both diurnal variation and daily average of soil temperature were larger at the south-facing slope than at the north-facing slope. As the canopy was closed up during the growing season, however, the difference became negligible. To include the topography effect on soil temperature, a comprehensive model which explains the spatial variation of daily radiative heat fluxes need to be incorporated into the hybrid model. Water content, colour, and texture of soil are also important factors causing errors in estimating soil temperature. The soil factors were implicitly considered in the hybrid model by soil thermal diffusivity, which might result in relative insensitivity of the hybrid model to the soil factors. In the case of wet soil condition or extremes in organic content or texture, an explicit way (e.g., numerical solution of the heat transfer equation) would be preferred.

One of the key questions in climate change research concerns the future dynamics of primary productivity and soil organic carbon. Kirshbaum (1995) reported much higher sensitivity of decomposition to increased temperature than that of net primary productivity, especially in low temperature range, suggesting a positive feedback in the global carbon cycle by elevated temperature. In fact, the hybrid model indicates that soil temperature is sensitive to rising air temperature at a low LAI level. Hence, it is hypothesized that global warming will give a more significant positive feedback on the global carbon cycle in a clear-cut area than in an uncut area at a local scale and in tundra than in temperate forests in a global scale since LAI is lower in tundra ($\approx 2 \, m^2 \, m^{-2}$) than in temperate forest (5–12 $m^2 \, m^{-2}$) (Whittaker and Likens, 1975). The hybrid model would be useful in evaluating this suggestion, incorporated into a well-established SOM model.

Land use change is also expected to affect the global carbon cycle by altering soil processes which are related to surface structure (Kauppi et al., 1992; Townsend and Vitousek, 1995; Mosier, 1998). In that sense, soil temperature is an environmental variable

that links surface structure to soil processes directly. This feature allows the hybrid model to be incorporated into other established models of soil organic matter and vegetation to predict spatially variable carbon cycle and its responses to land use change such as deforestation or reforestation.

Acknowledgements

References

Antonic, O., 1998. Modelling daily topographic solar radiation without site-specific hourly radiation data. Ecological Modelling 113, 31–40.

Becker, E.B., Carey, G.F., Oden, T., 1981. Finite elements: an introduction. Prentice-Hall, New Jersey.

Bellehumeur, C., Legendre, P., 1998. Multiscale sources of variation in ecological variables: modeling spatial dispersion, elaborating sampling designs. Landscape Ecology 13, 15–25.

Cressie, N.A.C., 1993. Statistics for Spatial Data. Wiley, New York, NY.

Daly, C., Neilson, R.P., Phillips, D.L., 1994. A statistical-topographic model for mapping climatological precipitation over mountainous terrain. J. Appl. Meteorol. 33, 140–158.

Deblonde, G., Penner, M., Royer, A., 1994. Measuring leaf index with the LI-COR LAI-2000 in pine stands. Ecology 75, 1507–1511.

Dozier, J., Frew, J., 1990. Rapid calculation of terrain parameters for radiation modeling from digital elevation data. IEEE Trans. Geosci. Remote Sens. 28, 963–969.

Dubayah, R., 1992. Estimating net solar radiation using Landsat Thematic mapper and Digital Elevation Data. Water Resources Research 28, 2469–2484.

Dubayah, R., 1994. Modeling a solar radiation topoclimatology for the Rio Grande River Basin. J. Veg. Sci. 5, 627–640.

Dubayah, R., Loechel, S., 1997. Modeling topographic solar radiation using GOES data. J. Appl. Meteorol. 36, 141–154.

Fassnacht, K.S., Gower, S.T., MacKenzie, M.D., Nordleim, E.V., Lillesand, T.M., 1997. Estimating the leaf area index of North Central Wisconsin Forests using the Landsat Thematic Mapper. Remote Sens. Environ. 61, 229–245.

Goovaerts, P., 1998. Geostatistical tools for characterizing the spatial variability of microbiological and physico-chemical soil properties. Biol. Fertil. Soils 27, 315–334.

Gower, S.T., Norman, J.M., 1991. Rapid estimation of leaf area index in conifer and broad-leaf plantations. Ecology 72, 1896–1900.

Goward, S.N., Waring, R.H., Dye, D.G., Yang, J., 1994. Ecological remote sensing at OTTER: satellite macroscale observations. Ecological Applications 4, 322–343.

Hudson, G., Wackernagel, H., 1994. Mapping temperature using kriging with external drift: theory and an example from Scotland. Int. J. Climatology 14, 77–91.

Hungerford, R.D., Nemani, R.R., Running, S.W., Coughlan, J.C., 1989. MTCLIM: a mountain microclimate simulation model. USDA Intermountain Research Station, Research Paper INT-414.

Iqbal, M., 1983. An introduction to solar radiation. Academic Press, NY.

Kauppi, P.E., Mielikainen, K., Kuusela, K., 1992. Biomass and carbon budget of European forests, 1971–1990. Science 256, 70–74.

Kimball, J.S., Running, S.W., Nemani, R., 1997. An improved method for estimating surface humidity from daily minimum temperature. Agric. and Forest Meteorol. 85, 87–98.

Kirshbaum, M.U.F., 1995. The temperature dependence of soil organic matter decomposition, and the effect of global warming on soil organic C storage. Soil Biol. Biochem. 27, 753–760.

Kitanidis, P.K., 1997. Introduction to Geostatistics. Cambridge University Press, New York, NY.

Kozlowski, T.T., Pallardy, S.G., 1997. Physiology of Woody Plants. Academic Press, San Diego.

Lee, D., Yoo, G., Oh, S., Shim, J.H., Kang, S., 1999. Significance of aspect and understory to leaf litter redistribution in a temperate hardwood forest. Korean J. Biol. Sci. 3, 143–147.

Marshall, T.J., Holmes, J.W., Rose, C.W., 1996. Soil physics, 3rd ed., Cambridge University Press, New York, NY.

Mosier, A.R., 1998. Soil processes and global change. Bio. Fertil. Soils 27, 221–229.

Monteith, J.L., Unsworth, M.H., 1990. Principles of environmental physics. Edward Arnold, A Division of Hodder and Stoughton, London.

Nemani, R., Running, S.W., 1996. Implementation of a hierarchical global vegetation classification in ecosystem function models. J. Vegetation Sci. 7, 337–346.

Pierce, L., Running, S.W., 1988. Rapid estimation of coniferous forest leaf area index using a portable integrating radiometer. Ecology 69, 1762–1767.

Raich, J.W., Schlesinger, W.H., 1992. The global carbon dioxide flux in soil respiration and its relationship to vegetation and climate, Tellus 44B, 81–99.

Rochette, P., Gregorich, E.G., 1998. Dynamics of soil microbial biomass C, Soluble organic C and CO_2 evolution after three years of manure application. Can. J. Soil Sci. 78, 283–290.

Rosenberg, N.J., Blad, B.L., Verma, S.B., 1983. Microclimate: The Biological Environment, 2nd ed., Wiley, New York, NY.

Russell, C.A., Voroney, R.P., 1998. Carbon dioxide efflux from the floor of a boreal aspen forest. I. Relationship to environmental variables and estimates of C respired. Can. J. Soil Sci. 78, 301–310.

Saha, S.K., 1995. Assessment of regional soil moisture conditions by coupling satellite sensor data with a soil–plant system heat and moisture balance model. Int. J. Remote Sens. 16, 973–980.

Spanner, M.A., Pierce, L.L., Peterson, D.L., Running, S.W., 1990. Remote sensing of temperate coniferous forest leaf area index: the influence of canopy closure, understory vegetation and background reflectance. Int. J. Remote Sens. 11, 95–111.

Striegl, R.G., Wickland, K.P., 1998. Effects of a clear-cut harvest on soil respiration in a jack pine-lichen woodland. Can. J. For. Res. 28, 534–539.

Thornton, P.E., Running, S.W., White, M.A., 1997. Generating surfaces of daily meteorological variables over large regions of complex terrain. J. Hydrology 190, 214–251.

Thunholm, B., 1990. A comparison of measured and simulated soil temperature using air temperature and soil surface energy balance as boundary condition. Agric. and Forest Meteorol. 53, 59–72.

Townsend, A.R., Vitousek, P.M., 1995. Soil organic matter dynamics along gradients in temperature and land use on the island of Hawaii. Ecology 76, 721–733.

Trumbore, S.E., Chadwick, O.A., Amundson, R., 1996. Rapid exchange between soil carbon and atmospheric carbon dioxide driven by temperature change. Science 272, 393–395.

Wackernagel, H., 1995. Multivariate Geostatistics. Springer, New York, NY.

Whittaker, R.H., Likens, G.E., 1975. The biosphere and man. In: Lieth, H., Whittaker, R.H. (Eds.), Primary Productivity of the Biosphere. Springer, Berlin, 306 pp.

Willmott, C.J., Robeson, S.M., 1995. Climatologically aided interpolation (CAI) of terrestrial air temperature. Int. J. Climatology 15, 214–229.

Yoo, G., Park, E., Kim, S., Lee, H., Kang, S., Lee, D., 1999. Transport and decomposition of leaf litter as affected by aspect and understory in a temperate hardwood forest, submitted to Forest Ecology and Management.

Zheng, D., Hunt Jr., E.R., Running, S.W., 1993. A daily soil temperature model based on air temperature and precipitation for continental applications. Climate Research 2, 183–191.

Zheng, D., Hunt Jr., E.R., Running, S.W., 1996. Comparison of available soil water capacity estimated from topography and soil series information. Landscape Ecology 11, 3–14.